Brief Communications

Ultra-High 7T MRI of Structural Age-Related Changes of the Subthalamic Nucleus

Max C. Keuken,[1,2] Pierre-Louis Bazin,[1] Andreas Schäfer,[1] Jane Neumann,[1,3] Robert Turner,[1] and Birte U. Forstmann[1,2]
[1]Max Planck Institute for Human Cognitive and Brain Sciences, 04103 Leipzig, Germany, [2]Cognitive Science Center Amsterdam, University of Amsterdam, 1018 WS Amsterdam, The Netherlands, and [3]Leipzig University Medical Center, IFB Adiposity Diseases, 04103 Leipzig, Germany

The subthalamic nucleus (STh) is a small subcortical structure which is involved in regulating motor as well as cognitive functions. Due to its small size and close proximity to other small subcortical structures, it has been a challenge to localize and visualize it using magnetic resonance imaging (MRI). Currently there are several standard atlases available that are used to localize the STh in functional MRI studies and clinical procedures such as deep brain stimulation (DBS). DBS is an increasingly common neurosurgical procedure that has been successfully used to alleviate motor symptoms present in Parkinson's disease. However, current atlases are based on low sample sizes and restricted age ranges (Schaltenbrand and Wahren, 1977), and hence the use of these atlases effectively ignores the substantial structural brain changes that are associated with aging. In the present study, ultra-high field 7 tesla (T) magnetic resonance imaging (MRI) in humans was used to visualize and segment the STh in young, middle-aged, and elderly participants. The resulting probabilistic atlas maps for all age groups show that the STh shifts in the lateral direction with increasing age. In sum, the results of the present study suggest that age has to be taken into account in atlases for the optimal localization of the STh in healthy and diseased brains.

Introduction

The subthalamic nucleus (STh) plays a key role in a range of motor and cognitive functions such as task switching (Mansfield et al., 2011), inhibition of ongoing behavior (Aron, 2007; Aron et al., 2007; Forstmann et al., 2012), and cognitive conflict (Cavanagh et al., 2011; Brittain et al., 2012; Zaghloul et al., 2012). The STh is a small subcortical structure and forms part of the basal ganglia (BG). Due to its small size and close proximity to structures such as the substantia nigra and the red nucleus, it has been a challenge to localize and visualize the STh (Mai and Paxinos, 2008).

An often-used atlas to localize the STh in surgical procedures and functional MRI is the human brain atlas from Schaltenbrand and Wahren (Schaltenbrand and Wahren, 1977; Starr, 2002). However, the disadvantage of this atlas is that only three brains with several consecutive slices were used to illustrate the BG (Schaltenbrand and Wahren, 1977; Vayssiere et al., 2002; Alho et al., 2011). Moreover, the three specimens were all male and the age range restricted (two specimens from 40-year-olds and one specimen from a 51-year-old at the time of death). Finally, the exact location of the STh differs across all three brains (Niemann and Van Nieuwenhofen, 1999). While other atlases of the STh are available, most suffer from similar problems which are (1) the restricted sample size, (2) the restricted age range, and (3) that they ignore the variability of location (Lucerna et al., 2002; Mai and Paxinos, 2008; Evans et al., 2012; Nakano et al., 2012).

The use of such atlases that do not incorporate the variability in the location frustrate the precise localization of the STh. Also it calls into question to what extent between-subject variability and within-subject age-related morphometric changes are taken into account when localizing the STh. Notably, den Dunnen and Staal (2005) showed that the location of the STh changes with age. By measuring the location of the STh in 12 postmortem brains (age range 29–85 years), the authors found that increasing age causes the STh to shift in superior, lateral, and anterior directions. Kitajima et al. (2008) report a similar lateral shift of the STh for *in vivo* data measured with 3T MRI. However, a recent paper by Massey et al. (2012) came to a different conclusion. Based on a sample of eight postmortem brains (age range 38–95 years), no relationship between the age at death and STh location was found. In sum, until now it has remained unclear whether there is a shift in location and possibly changes in volume of the STh in the aging brain.

In the present study, healthy young, middle-aged, and elderly participants were scanned on an ultra-high field 7T MRI scanner. Using ultra-high resolution 7T MRI, it is possible to investigate a shift in location of the STh *in vivo* related to aging. Both a shift in location as well as changes in STh volume have important implications for surgical procedures and the localization of the STh in general.

Materials and Methods

Participants. Thirteen young participants were scanned, with an average age of 24.38 years (age range: 22–28 years, SD 2.36; six females). In addition, nine middle-aged participants with an average age of 50.67 years (age range 40–59 years; SD 6.63; five females), and nine elderly

Received July 8, 2012; revised Jan. 12, 2013; accepted Jan. 25, 2013.

Author contributions: M.C.K. and B.U.F. designed research; M.C.K. and A.S. performed research; P.-L.B. and R.T. contributed unpublished reagents/analytic tools; M.C.K., P.-L.B., and J.N. analyzed data; M.C.K., P.-L.B., A.S., J.N., R.T., and B.U.F. wrote the paper.

This work was supported by a VENI (BUF) grant from the Netherlands Organization for Scientific Research. We thank Domenica Wilfling and Elisabeth Wladimirow as well as Siemens Medical Solutions.

This article is freely available online through the *J Neurosci* Open Choice option.

Correspondence should be addressed to Max C. Keuken, Nieuwe Achtergracht 129, 1018 WS Amsterdam, The Netherlands. E-mail: mckeuken@gmail.com.

DOI:10.1523/JNEUROSCI.3241-12.2013

 0270-6474/13/334896-05$15.00/0

Table 1. Mean volume (SD) in cubic millimeters of the inter-rater STh masks for the left and right hemisphere separately for the three age groups

	Left	Right
Young	67.55 mm^3 (25.89)	57.20 mm^3 (20.66)
Middle-aged	77.25 mm^3 (20.99)	73.68 mm^3 (19.77)
Elderly	51.58 mm^3 (23.31)	52.22 mm^3 (30.27)

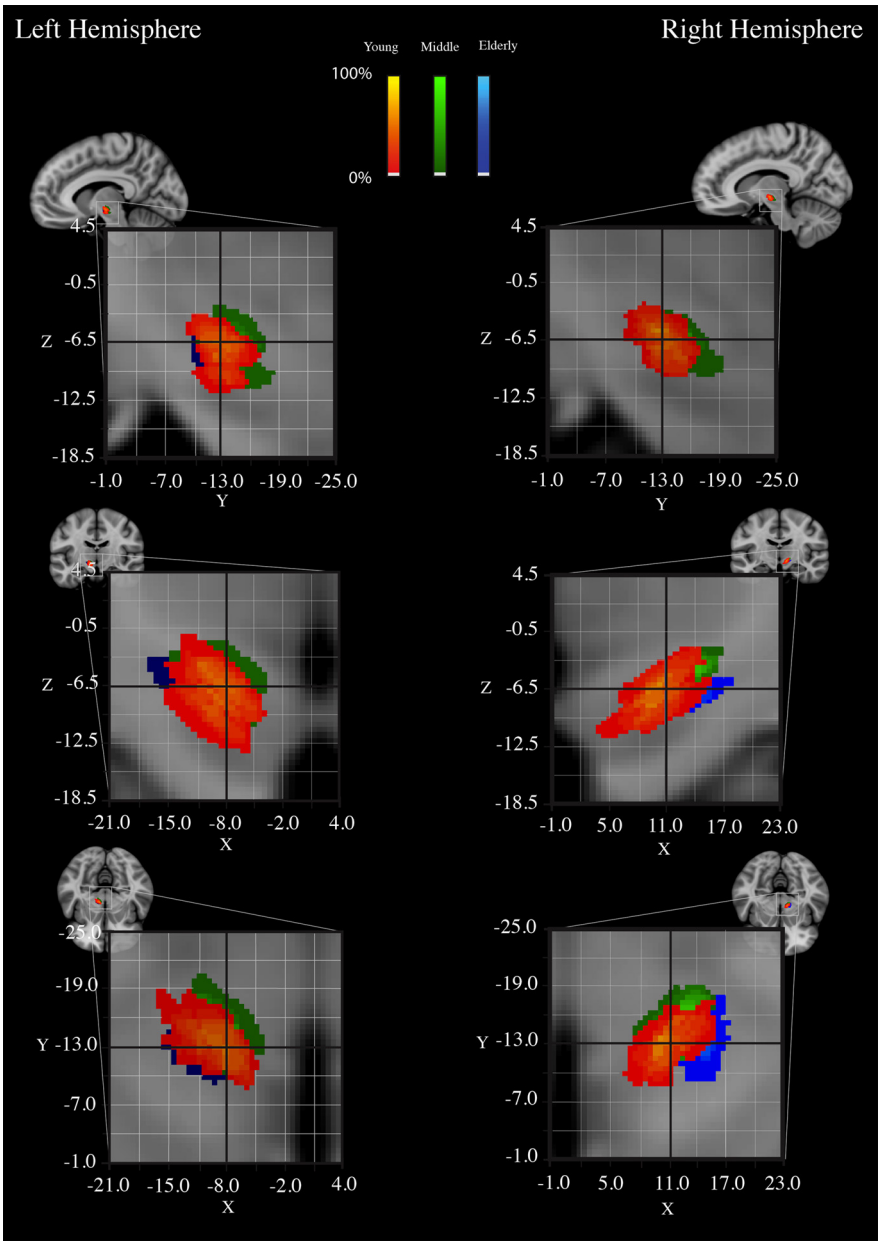

Figure 1. The overlap among the three age groups of the STh probabilistic maps based on the inter-rater masks. The probability maps for the young participants are displayed in red-yellow. The probability maps for the middle-aged participants are displayed in green. The probability maps for the elderly participants are displayed in blue. Color intensity reflects the percentage overlap between individuals.

participants were scanned. The elderly participants were on average 72.33 years old (age range 67–77 years; SD 2.87; four females). None of the participants had a history of neurological disorders or suffered from psychiatric disorders. The study was approved by the local ethical committee of the Max Planck Institute for Human Brain and Cognitive Sciences in Leipzig. All participants gave written informed consent.

Data acquisition of ultra-high resolution anatomical images. All participants underwent structural scanning on a 7T Magnetom MRI system (Siemens, Erlangen) using a 24-channel head array Nova coil (NOVA Medical Inc., Wilmington MA). Whole-brain images were acquired with an MP-RAGE sequence (TR = 3000 ms, TE = 2.95 ms, TI = 1100 ms, voxel size: 0.8 mm^3, flip angle = 6°, GRAPPA acceleration factor 2) for the young and elderly group. For the middle-aged group the whole-brain images were acquired with an MP2RAGE sequences (TR = 5000 ms, TE = 2.45 ms, TI = 900/2750 ms, voxel size: 0.7 mm^3, flip angle = 5/3°, GRAPPA acceleration factor 2). Moreover, a multi echo spoiled 3 dimensional (3D) gradient echo (FLASH) sequence (TR = 43 ms, TE = 11.22 ms, TE = 21.41 ms, TE = 31.59 ms, flip angle = 13°, voxel 0.5, 0.5, 0.6 mm, 56 coronal slices) was acquired (for more detailed information about the scan sequence see Forstmann et al., 2012).

Manual segmentation of the STh. Manual segmentation was performed using the FSL 4.1.4 viewer (http://fsl.fmrib.ox.ac.uk/fsl/fslwiki/). Segmentation was performed by two independent researchers and inter-rater agreement was assessed. For more detailed information regarding the segmentation protocol see Forstmann et al. (2012). The FLASH sequence for one of the middle-aged participants contained severe motion artifacts which made it impossible to distinguish the STh and as a consequence this participant was excluded from the data analyses. Only voxels rated by both raters as belonging to the STh were included in any further analyses. Finally, inter-rater reliability (young: mean/SD of Cohen's $\kappa = 0.86/0.05$; middle-aged: mean/SD of Cohen's $\kappa = 0.61/0.10$; elderly: mean/SD of Cohen's $\kappa = 0.61/0.15$) were calculated. Due to unknown factors, the distinction of the STh from the SN was lower for the middle-aged and elderly participants compared with the young participants. Therefore the STh for the middle-aged participants were segmented twice and the data of the elderly participants were segmented three times in total. Only the last segmentation was used for further processing. There was a main effect of inter-rater values between age groups ($F_{(2)} = 7.41$, $p = 0.001$). *Post hoc* analyses revealed lower inter-rater values for middle-aged and elderly participants compared with the young participants (young vs middle-aged: $p = 0.005$; young vs elderly: $p = 0.006$, corrected for multiple comparisons using Tukey HSD).

A possible cause for the reduced inter-rater values for the middle-aged and elderly participants could be a different local increase in iron in both the STh and SN with age. This increase blurs the borders between both structures possibly inducing variability. This explanation is in line with work of Aquino et al. (2009) showing that the level of iron in the SN stabilizes at the age of 25. In addition, the work of Schäfer et al. (2012) revealed that the T2* values of the SN, measured with a magnetic field strength of 7T, is on average 14 ms for the young participants. In sum, it appears that the T2* value of the STh and SN in the middle-aged and elderly participants are more comparable than in the young participants possibly hampering a clear distinction between the two structures.

To test this hypothesis, the mean T2* value which is thought to reflect the level of iron (Schenck, 2003; Aquino et al., 2009; Schäfer et al., 2012) was calculated and extracted for every individual STh. There was a main effect of age group on the mean T2* values of the STh ($F_{(2)} = 15.26$, $p <$

0.001).The middle-aged and elderly participants had a lower mean T2* STh value compared with the young participants (young vs middle-aged: $p = 0.000$, young vs elderly: $p = 0.001$, middle-aged vs elderly: $p = 0.23$, corrected for multiple comparison using Tukey HSD). The mean T2* values of the STh for the young participants was 17.22 ms (SD 0.26), middle-aged 14.56 ms (SD 0.35), and elderly participants 15.44 ms (SD 0.46). Finally the mean T2* values of the STh correlated with the inter-rater Cohen's κ ($r_{(56)} = 0.35, p = 0.006$). To ensure that the decrease in T2* across age groups has no effect on the volume estimation or shift of the STh with increasing age, the T2* values are always taken into account by using partial correlations.

Computation of probability maps and atlasing of the STh. The STh masks were delineated in the acquisition space of the T2*-weighted FLASH images which covered a thin region oriented coronally and centered on the subthalamic region. To register these masks to MNI standard space, the FLASH image was first aligned to the MP(2)RAGE image of the same participant. In a next step, the individual MP(2)RAGE was registered to standard space. Finally, the original FLASH images and the masks were directly transformed to standard space by using the two transformation matrices. Due to B1 inhomogeneities at 7T, the registration from FLASH to MPRAGE required a semiautomated approach based on landmark correspondence. First, the following landmarks on the anatomy were identified: the posterior commissure, the top indentation of the pons, the start of the trigeminal nerves out of the brainstem, left and right, and the top of the crux of the fornix. Landmark identifications were performed in triplanar views displaying both images simultaneously in the MIPAV software package (http://mipav.cit.nih.gov). Second, the FLASH STh mask image was transferred into subject space with a rigid transformation estimated from the landmarks. All landmark-based registration results have been visually checked, and the entire procedure repeated if any misalignment could be detected to the region of the STh. To compensate for interpolation in these small structures, the signed distance function for each of the masks were computed first and transferred, and the final delineation was obtained by thresholding the transformed function. Once all the delineations were in MNI space, a statistical atlas was generated by averaging the masks.

Given the small size of the STh, the multiple registration steps, and the anatomical variability, the statistical atlas was checked for outliers by comparing the average probability for each delineated mask with each individual STh mask. This resulted in discarding one young participant from all analyses because the participant fell below 1 SD compared with the rest of the young participants. Note that this is the same participant who was also excluded in the full registration procedure as described by Forstmann et al. (2012).

The young, middle-aged, and elderly MNI probabilistic masks have been made publicly available (http://www.nitrc.org/projects/atag/). Note that the probabilistic maps are different from the standard maps included in FSL (http://fsl.fmrib.ox.ac.uk/fsl/fslwiki/Atlases or http://www.nitrc.org/projects/atag), which are based on the full registration procedure (landmark-based and automated) and only the young subjects (see Forstmann et al., 2012 for details).

Calculation of location. To determine the location of the STh, we calculated the center of mass (CoM) of the inter-rater masks of each STh using FSLUTILS as implemented in the FSL software package. Thereby no prior assumptions were made about the shape or mean relative distance of the boundary of the STh to other structures.

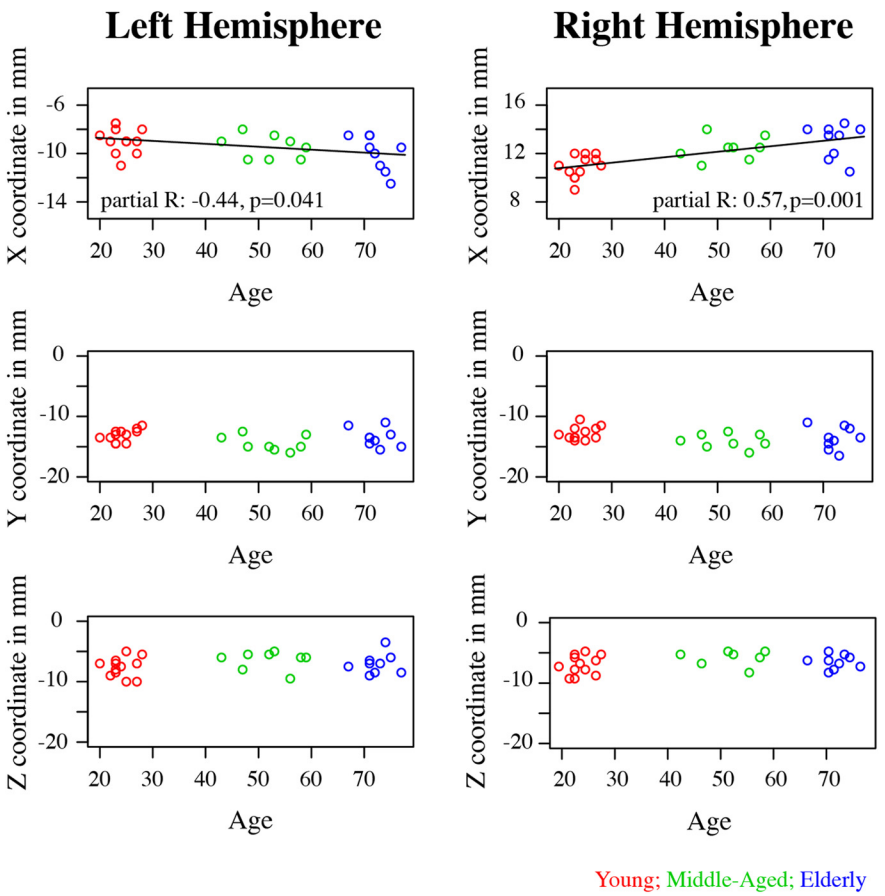

Figure 2. Top row, The *X* CoM coordinates of the STh masks in millimeters. Middle row, The *Y* CoM coordinates of the STh masks. Bottom row, The *Z* CoM coordinates of the STh masks. The young masks are plotted in red; the middle-aged masks are plotted in green; the elderly masks are plotted in blue.

Results

Volume of the STh

The volume of the STh was calculated in individual space by using the inter-rater masks and only incorporate voxels that both raters agreed on (see Table 1 for the results).

Based on an ANOVA there was no effect of hemisphere on STh volume ($F_{(1)} = 0.60, p = 0.44$). A partial correlation between age and STh volume controlling for mean T2* differences in the STh was computed. No significant relation was found ($t_{(58)} = -1.89, p = 0.057$).

Location of the STh

Based on the registration to MNI space for young, middle-aged, and elderly participants, there was some overlap among the three age groups (Fig. 1).

However, when quantifying the spatial distance of the CoM coordinate, the groups differed significantly in spatial location. By correlating the *X*, *Y*, and *Z* MNI coordinates (respectively, sagittal, coronal, and axial directions) separately for each hemisphere with age, while controlling for T2* values, we found that the *X* dimension correlated highly with age (left hemisphere: $r_{(27)} = -0.44, p = 0.041$; right hemisphere: $r_{(27)} = 0.57, p = 0.001$), corrected for multiple comparisons using a Bonferroni correction). The correlation revealed that there is a shift of STh

location in a lateral direction with increasing age (Fig. 2). No significant correlation between location and age was found for either the *Y* or *Z* direction.

As proposed by Kitajima et al. (2008), a possible cause for such a shift could be an increase of the ventricles and specifically the third ventricle. To test this hypothesis, the lateral, aqueduct, third, and fourth ventricle were manually segmented in individual space separately for each participant and hemisphere. Once the ventricles were segmented, the volumes were extracted and tested with a paired *t* test to test for differences between hemispheres. There were no significant differences between hemispheres for the lateral ventricle volume over age groups ($F_{(1)} = 0.02$, $p = 0.88$). Overall, the total ventricle size increased with increasing age reflected by a significant correlation of $r = 0.68$ ($t_{(56)} = 6.80$, $p < 0.001$).

Based on the CoM coordinate, differences between the age groups, we first investigated whether a relationship exists between the shift of the STh and the total size of the ventricle system. By correlating the *X*, *Y*, and *Z* MNI coordinates with the total ventricle size for each hemisphere separately, we found that the *x*-axis center of mass coordinate of the STh correlated highly with the ventricle volume (left hemisphere: $r_{(27)} = -0.42$, $p = 0.023$; right hemisphere: $r_{(27)} = 0.67$, $p < 0.001$). There was no significant correlation between the total ventricle volume and the *y*-axis or *z*-axis center of mass coordinate of the STh. However, when controlling for age, no significant correlation was found between total ventricle size and *x*-axis CoM coordinate (left hemisphere: $r_{(27)} = -0.28$, $p = 0.40$; right hemisphere: $r_{(27)} = 0.33$, $p = 0.23$, corrected for multiple comparisons using a Bonferroni correction). This result indicates that the total ventricle size does not explain more variance compared with the variance explained by age alone.

More specifically, to test whether the third ventricle alone could explain the lateral shift of the STh, we first computed a correlation between the volume of the third ventricle and age (correlation of 0.77 ($t_{(56)} = 8.93$, $p < 0.001$). In addition, we computed partial correlations between third ventricle volume and *X* location of the STh controlling for age. Again, no significant correlation was found (left hemisphere: $r_{(27)} = -0.17$, $p = 1$; right hemisphere: $r_{(27)} = 0.40$, $p = 0.07$, corrected for multiple comparisons using a Bonferroni correction).

Discussion

Are there age-related changes in location and volume in the STh? In the present study, young, middle-aged, and elderly participants were structurally scanned using ultra-high resolution 7T MRI. In line with previous postmortem work by den Dunnen and Staal (2005) (see their Fig. 3) and *in vivo* work by Kitajima et al. (2008), the results clearly indicate that the location of the STh shifts in the lateral direction with increasing age. However, no significant decrease in STh volume was detected despite a large body of literature showing that healthy aging is accompanied by structural gray matter changes (Raz and Rodrigue, 2006; Fjell and Walhovd, 2010). A possible explanation for the current finding is the age range of our elderly sample. The oldest participant was 77 years old, while certain structural changes may only occur at a later stage in life [Barron et al., 1976; Cherubini et al., 2009; but see also Massey et al. (2012), who, investigating a broader age range, also failed to find a decrease in STh volume associated with age].

Importantly, the present results showed a significant change in location of the STh in the elderly compared with the younger participants. This finding is in line with previous work (den Dunnen and Staal, 2005; Kitajima et al., 2008). A possible explanation for this lateral shift is the enlargement of ventricles with increasing age which might be due to the loss of white matter tissue (Guttmann et al., 1998; Fjell and Walhovd, 2010). The results clearly indicate a positive correlation between volume of ventricles and age. However, when controlling for age, there is no significant correlation found between the enlargement of ventricles and the lateral shift of the STh. Unfortunately, the lack of diffusion-weighted imaging in the current study does not allow the investigation of changes in white matter tissue in, e.g., the internal capsule (Kawaguchi et al., 2010), as a possible reason to explain the lateral shift of the STh.

Finally, the present results point to the fact that between-subject variability and within-subject age-related brain changes should be taken into account for new generation atlases (Evans et al., 2012). For more than two decades, the severe motor symptoms of Parkinson's Disease (PD) have been alleviated using deep brain stimulation (DBS) (Limousin et al., 1995). DBS in PD requires a surgical procedure in which a microelectrode is lowered into the STh to induce electrical stimulation (Perlmutter and Mink, 2006; Limousin and Martinez-Torres, 2008). Common neurosurgical practice in deciding where to place the DBS microelectrodes is to superimpose an anatomical MRI of the patient to a normalized standard atlas diagram (Abosch et al., 2010). Note that current atlases for the STh that are used for surgical procedures are based on low sample sizes, a very restricted age range, and low field MRI (Schaltenbrand and Wahren, 1977; Lucerna et al., 2002; Mai and Paxinos, 2008; Nakano et al., 2012). Because PD is diagnosed at an increasingly early age (Shulman et al., 2011), and the possibility to implant DBS electrodes is at an increasing broad age range (Kleiner-Fisman et al., 2006; Parent et al., 2011), a mismatch between the current atlas coordinates and the actual location of the target structure appears likely. A possible consequence could be a heightened occurrence of highly undesirable side effects such as a decline in cognitive functioning, whereas others experience depression, hypermania, hypersexuality, and in some extreme cases, commit suicide (Burkhard et al., 2004; Temel et al., 2005).

In sum, a higher level of clinical efficacy might be achieved by providing atlases that incorporate individual differences (cf. Forstmann et al., 2012), account for age-related changes (cf. Habas et al., 2009), possibly disease-specific brain changes, and are based on ultra-high field MRI (e.g., 7T). The increase in signal-to-noise and decrease in isotropic voxel size available at ultra-high field MRI is essential to study small structures like the STh (Cho et al., 2008, 2010; Abosch et al., 2010; Beisteiner et al., 2011).

References

Abosch A, Yacoub E, Ugurbil K, Harel N (2010) An assessment of current brain targets for deep brain stimulation surgery with susceptibility-weighted imaging at 7 tesla. Neurosurgery 67:1745–1756. CrossRef Medline

Alho E, Grinberg L, Heinsen H (2011) Review of printed and electronic stereotactic atlases of the human brain. In: Neuroimaging for clinicians—combining research and practice (Peres JFP, ed). New York: InTech.

Aquino D, Bizzi A, Grisoli M, Garavaglia B, Bruzzone MG, Nardocci N, Savoiardo M, Chiapparini L (2009) Age-related iron deposition in the basal ganglia: quantitative analysis in healthy subjects. Radiology 252: 165–172. CrossRef Medline

Aron AR (2007) The neural basis of inhibition in cognitive control. Neuroscientist 13:214–228. CrossRef Medline

Aron AR, Behrens TE, Smith S, Frank MJ, Poldrack RA (2007) Triangulating a cognitive control network using diffusion-weighted magnetic resonance imaging (MRI) and functional MRI. J Neurosci 27:3743–3752. CrossRef Medline

Barron SA, Jacobs L, Kinkel WR (1976) Changes in size of normal lateral ventricles during aging determined by computerized tomography. Neurology 26:1011–1013. CrossRef Medline

Beisteiner R, Robinson S, Wurnig M, Hilbert M, Merksa K, Rath J, Höllinger I, Klinger N, Marosi Ch, Trattnig S, Geissler A (2011) Clinical fMRI: evidence for a 7T benefit over 3T. Neuroimage 57:1015–1021. CrossRef Medline

Brittain JS, Watkins KE, Joundi RA, Ray NJ, Holland P, Green AL, Aziz TZ, Jenkinson N (2012) A role for the subthalamic nucleus in response inhibition during conflict. J Neurosci 32:13396–13401. CrossRef Medline

Burkhard PR, Vingerhoets FJG, Berney A, Bogousslavsky J, Villemure JG, Ghika J (2004) Suicide after successful deep brain stimulation for movement disorders. Neurology 63:2170–2172. CrossRef Medline

Cavanagh JF, Wiecki TV, Cohen MX, Figueroa CM, Samanta J, Sherman SJ, Frank MJ (2011) Subthalamic nucleus stimulation reverses mediofrontal influence over decision threshold. Nat Neurosci 14:1462–1467. CrossRef Medline

Cherubini A, Péran P, Caltagirone C, Sabatini U, Spalletta G (2009) Aging of subcortical nuclei: Microstructural, mineralization and atrophy modifications measured in vivo using MRI. Neuroimage 48:29–36. CrossRef Medline

Cho ZH, Kim YB, Han JY, Min HK, Kim KN, Choi SH, Veklerov E, Shepp LA (2008) New brain atlas—mapping the human brain in vivo with 7.0 T MRI and comparison with postmortem histology: Will these images change modern medicine? Int J Imaging Syst Technol 18:2–8. CrossRef

Cho ZH, Min HK, Oh SH, Han JY, Park CW, Chi JG, Kim YB, Paek SH, Lozano AM, Lee KH (2010) Direct visualization of deep brain stimulation targets in Parkinson disease with the use of 7-tesla magnetic resonance imaging. J Neurosurg 113:639–647. CrossRef Medline

den Dunnen WF, Staal MJ (2005) Anatomical alterations of the subthalamic nucleus in relation to age: A postmortem study. Movement Disorders 20:893–898. CrossRef Medline

Evans AC, Janke AL, Collins DL, Baillet S (2012) Brain templates and atlases. Neuroimage 62:911–922. CrossRef Medline

Fjell AM, Walhovd KB (2010) Structural brain changes in aging: courses, causes and cognitive consequences. Rev Neurosci 21:187–221. Medline

Forstmann BU, Keuken MC, Jahfari S, Bazin PL, Neumann J, Schäfer A, Anwander A, Turner R (2012) Cortico-subthalamic white matter tract strength predict interindividual efficacy in stopping a motor response. Neuroimage 60:370–375. CrossRef Medline

Guttmann CRG, Jolesz FA, Kikinis R, Killiany RJ, Moss MB, Sandor T, Albert MS (1998) White matter changes with normal aging. Neurology 50:972–978. CrossRef Medline

Habas P, Kim K, Rousseau F, Glenn O, Barkovich A, Studholme C (2009) A spatio-temporal atlas of the human fetal brain with application to tissue segmentation. Med Image Comput Comput Assist Interv 2009 12:289–296.

Kawaguchi H, Obata T, Ota M, Akine Y, Ito H, Ikehira H, Kanno I, Suhara T (2010) Regional heterogeneity and age-related change in subregions of internal capsule evaluated by diffusion tensor imaging. Brain Res 1354:30–39. CrossRef Medline

Kitajima M, Korogi Y, Kakeda S, Moriya J, Ohnari N, Sato T, Hayashida Y, Hirai T, Okuda T, Yamashita Y (2008) Human subthalamic nucleus: evaluation with high-resolution MR imaging at 3.0 T. Neuroradiology 50:675–681. CrossRef Medline

Kleiner-Fisman G, Herzog J, Fisman DN, Tamma F, Lyons KE, Pahwa R, Lang AE, Deuschl G (2006) Subthalamic nucleus deep brain stimulation: summary and meta-analysis of outcomes. Movement Disorders 21:S290–S304. CrossRef Medline

Limousin P, Martinez-Torres I (2008) Deep brain stimulation for Parkinson's disease. Neurotherapeutics 5:309–319. CrossRef Medline

Limousin P, Pollak P, Benazzouz A, Hoffmann D, Le Bas JF, Broussolle E, Perret JE, Benabid AL (1995) Effect of parkinsonian signs and symptoms of bilateral subthalamic nucleus stimulation. Lancet 345:91–95. CrossRef Medline

Lucerna S, Salpietro FM, Alafaci C, Tomasello F (2002) In vivo atlas of deep brain structures: with 3D reconstructions. New York: Springer.

Mai JK, Paxinos G (2008) Atlas of the Human Brain, Ed 3. San Diego: Academic.

Mansfield EL, Karayanidis F, Jamadar S, Heathcote A, Forstmann BU (2011) Adjustments of response threshold during task switching: a model-based functional magnetic resonance imaging study. J Neurosci 31:14688–14692. CrossRef Medline

Massey LA, Miranda MA, Zrinzo L, Al-Helli O, Parkes HG, Thornton JS, So PW, White MJ, Mancini L, Strand C, Holton JL, Hariz MI, Lees AJ, Revesz T, Yousry TA (2012) High resolution MR anatomy of the subthalamic nucleus: imaging at 9.4T with histological validation. Neuroimage 59:2035–2044. CrossRef Medline

Nakano N, Taneda M, Watanabe A, Kato A (2012) Computed three-dimensional atlas of subthalamic nucleus and its adjacent structures for deep brain stimulation in Parkinson's disease. ISRN Neurology 2012:592678. CrossRef Medline

Niemann K, Van Nieuwenhofen I (1999) One atlas—three anatomies: relationships of the Schaltenbrand and Wahren microscopic data. Acta Neurochir 141:1025–1038. CrossRef

Parent B, Awan N, Berman SB, Suski V, Moore R, Crammond D, Kondziolka D (2011) The relevance of age and disease duration for intervention with subthalamic nucleus deep brain stimulation surgery in Parkinson disease. J Neurosurg 114:927–931. CrossRef Medline

Perlmutter JS, Mink JW (2006) Deep brain stimulation. Annual Rev Neurosci 29:229–257. CrossRef

Raz N, Rodrigue KM (2006) Differential aging of the brain: Patterns, cognitive correlates and modifiers. Neurosci Biobehav Rev 30:730–748. CrossRef Medline

Schäfer A, Forstmann BU, Neumann J, Wharton S, Mietke A, Bowtell R, Turner R (2012) Direct visualization of the subthalamic nucleus and its iron distribution using high-resolution susceptibility mapping. Hum Brain Mapp 33:2831–2842. CrossRef Medline

Schaltenbrand G, Wahren W (1977) Introduction to stereotaxis with an atlas of the human brain. Stuttgart: Thieme.

Schenck JF (2003) Magnetic resonance imaging of brain iron. J Neurol Sci 207:99–102. CrossRef Medline

Shulman JM, De Jager PL, Feany MB (2011) Parkinson's disease: genetics and pathogenesis. Annu Rev Pathol Mech Dis 6:193–222. CrossRef

Starr PA (2002) Placement of deep brain stimulators into the subthalamic nucleus or globus pallidus internus: technical approach. Stereotact Funct Neurosurg 79:118–145. CrossRef Medline

Temel Y, Blokland A, Steinbusch HW, Visser-Vandewalle V (2005) The functional role of the subthalamic nucleus in cognitive and limbic circuits. Prog Neurobiol 76:393–413. CrossRef Medline

Vayssiere N, Hemm S, Cif L, Picot MC, Diakonova N, El Fertit H, Frerebeau P, Coubes P (2002) Comparison of atlas-and magnetic resonance imaging-based stereotactic targeting of the globus pallidus internus in the performance of deep brain stimulation for the treatment of dystonia. J Neurosurg 96:673–679. CrossRef Medline

Zaghloul KA, Weidemann CT, Lega BC, Jaggi JL, Baltuch GH, Kahana MJ (2012) Neuronal activity in the human subthalamic nucleus encodes decision conflict during action selection. J Neurosci 32:2453–2460. CrossRef Medline